PHYSICAL REVIEW B **75**, 205422 (2007)

Host-guest interaction effect on electron transport in disordered network of nanographite domains

K. Sugihara
1-40-6-506, Shibayama, Funabashi City, Chiba 274-0816, Japan

K. Takahara, K. Takai, and T. Enoki
Department of Chemistry, Tokyo Institute of Technology, 2-12-1, Ookayama, Meguro-ku, Tokyo 152-8551, Japan

(Received 6 September 2006; revised manuscript received 26 January 2007; published 16 May 2007)

Nanosized graphite (nanographite) is unique carbon material with localized spins originating from the nonbonding π-electron state (edge-state) on their edge sites instead of the diamagnetic properties of bulk-sized graphite. Activated carbon fibers (ACFs) consist of a three-dimensional disordered network of nanographite metallic domains and have large specific surface areas due to the presence of nanosized pores (nanopores). The electron transport in ACFs can be explained by the Coulomb-gap-type variable hopping between nanographite domains, and it exhibits a large positive magnetoresistance at low temperatures. This magnetoresistance decreases significantly upon magnetic oxygen adsorption, in spite of its insensitivity to nonmagnetic molecular species such as nitrogen, argon, and helium. This result suggests the presence of a strong interaction between the oxygen molecule spin and edge-state spin. The strong effect of oxygen adsorption on magnetotransport is theoretically explained in terms of the interaction between the electric dipole moment of the edge-state π-electron and electric quadrupole moment of the adsorbed oxygen molecule. Theoretical calculation reproduces the experimentally reported strength of the exchange interaction between the oxygen molecule spin and edge-state spin, in addition to the behavior of the magnetoresistance.

DOI: 10.1103/PhysRevB.75.205422 PACS number(s): 73.63.−b, 72.10.Bg, 75.47.−m

I. INTRODUCTION

Fujita *et al.* opened a new horizon in the research on disordered nanographene with their proposed theory on the edge-shape effect on the electronic structure of nanographite.[1,2] The most important contribution of their work was the clarification of the edge-shape dependence of the electronic structure of nanographene ribbons. The electronic structures of nanographene in the case of armchair- and zigzag-shaped edges differ completely. In the former case, the electronic structure of nanographene is the same as that of two-dimensional bulk-sized graphite with the continuous thickening of the nanographene ribbon width. At $k=0$, the bottom of the π^*-conduction band and top of the π-valence band degenerate, thereby resulting in $E(k)$ being linear with respect to k. In the latter case, a dispersionless band, which is attributed to the nonbonding π-electron state (edge state), appears around the Fermi energy in the region of the wave number $2\pi/3 \leqslant |k| \leqslant \pi$. Due to the survival of this band at the hydrogen-terminated edge, it originates not from the σ-dangling bond but from the nonbonding π-orbital localized around the zigzag edge. In particular, at $|k|=\pi$, the state is completely localized along the zigzag-edge sites with its wave function decaying into the interior of the nanographene ribbon as k approaches $2\pi/3$.

In recent studies, the presence of an edge state on hydrogen-terminated zigzag-shaped graphene edges has been confirmed experimentally by scanning tunneling microscopy and spectroscopy.[3–5] The edge states localized around the graphene edge region have localized spins that interact with the π-conduction electrons. This is similar to the *s*-*d* interaction in traditional metal magnets. Therefore, edge-state spins are considered to be the building blocks for designing carbon-only magnetic systems. In fact, the ferromagnetism of edge-state spins is theoretically predicted.[6] They are also a key ingredient in cooperative phenomena such as the Kondo effect,[7] giant magnetoresistance effect,[8] etc., which are governed by the interaction of conduction electrons with localized spins.

Activated carbon fibers (ACFs) are one of the important nanographite-based materials used for examining the anomalous electronic and magnetic features of nanographites in which edge-state π electrons play an important role. ACFs consist of a three-dimensional disordered network of nanographite metallic domains, each of which is a stack of three to four nanographene sheets with a mean in-plane size of 2–3 nm. According to previous studies,[9,10] the presence of edge-state spins induces an anomalous electron transport phenomenon, i.e., ACFs exhibit a large positive magnetoresistance at low temperatures[11] the value of which approaches almost 670% at 15 T and 2 K (Ref. 12). This phenomenon can be explained in terms of the interaction between the edge-state spin and π-conduction electron (described later). In addition, the nanopores surrounded by nanographite domains, which provide large specific surface areas ($\sim$2000 $\mathrm{m}^2\,\mathrm{g}^{-1}$), can accommodate a large volume of guest species through physisorption and chemisorption processes. It is reported that molecular adsorption strongly affects electronic and magnetic properties,[12–16] even when the physisorption driven by van der Waals interaction is responsible for the adsorption mechanism. It is observed that the significant condensation of helium at room temperature accelerates the dissipation of energy from the edge-state spins to the environment.[13,17] Moreover, physisorbed guest molecules

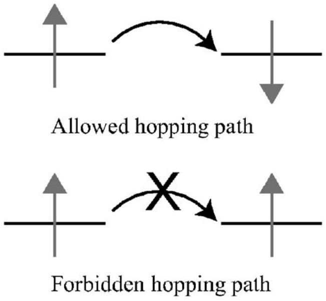

FIG. 1. Allowed and forbidden hopping paths depending on the spin orientation between the edge-state spins on adjacent nanographite domains.

induce a transition from the high spin state to low spin state in the edge-state spins through the adsorption-induced structural change.[15] In the case of molecular adsorption in ACF nanopores, the study of magnetic oxygen molecules, which have localized spins ($S=1$), yield interesting results. Interestingly, our recent study revealed that the adsorption of magnetic oxygen molecules significantly reduces magnetoresistance (ca. 40%), in spite of its insensitivity to nonmagnetic molecular species.[12]

It is considered that the conduction mechanism in ACF nanographite networks differs from that of the impurity band of conventional semiconductors, which have shallow-impurity bands. The electron hopping process between nanographite domains, wherein the interdomain wave-function overlap is relatively small, plays a critically important role in this mechanism. In fact, the anomalous large positive magnetoresistance can be explained by the spin-polarization effect in the hopping process,[12,18,19] i.e., the spin of the electron allowed to hop from a nanographite domain to the one adjacent to it is required to be antiparallel to the spin of the electron that was in the adjacent domain, as shown in Fig. 1. The significant change in magnetoresistance induced by oxygen uptake is attributed to the antiferromagnetic internal field of oxygen molecules. The adsorption of magnetic oxygen molecules reduces the effective field acting on the edge-state spins by the compensation of the external field by the antiferromagnetic internal field of oxygen molecules. This mechanism indicates that there exists a strong antiferromagnetic interaction between the oxygen molecule spin and edge-state spin in nanographite domain. Based on the analysis of the experimental result, the magnetic interaction is estimated to be -6 to -8 K (Ref. 12). The strength of the interaction cannot be explained by considering only the magnetic dipole-dipole interaction, which plays a major role in ordinary physisorbed systems.

The objective of this study is to clarify the microscopic mechanism of the electron hopping process between nanographites with regard to the anomalous magnetotransport observed in nanographite networks and its molecular adsorption effect, based on the experimental data provided in Ref. 12. Sections II and III describe the microscopic origin of the interaction between the oxygen molecule spin and edge-state spin and mechanism of the hopping process between nanographite domains, respectively.

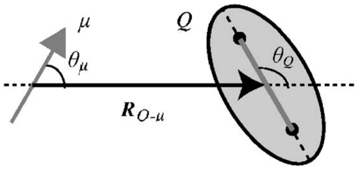

FIG. 2. Electric dipole-quadrupole interaction between the edge-state spin and oxygen molecule spin. μ, Q, $\boldsymbol{R}_{\text{Q-}\mu}$, θ_Q, and θ_μ are the electric dipole on the edge-site of a nanographite, electric quadrupole moment of an oxygen molecule, distance vector between the centers of the electric dipole μ and electric quadrupole Q, angle formed by the intersection of the molecular axis of oxygen with vector $\boldsymbol{R}_{\text{Q-}\mu}$, and angle formed by μ with vector $\boldsymbol{R}_{\text{Q-}\mu}$, respectively.

II. ORIGIN OF THE EFFECTIVE FIELD INDUCED BY OXYGEN MOLECULE SPINS

Takahara *et al.*[12] explained the oxygen-adsorption-induced decrease in magnetoresistance on the basis of the exchange coupling $-2z_{\pi\text{-Ox}}J_{\pi\text{-Ox}}\boldsymbol{s}\cdot\boldsymbol{S}$ between an oxygen molecule spin $\mathbf{S}$ and edge-state spin $\boldsymbol{s}$. Here, $z_{\pi\text{-Ox}}$ and $J_{\pi\text{-Ox}}$ are the number of nearest-neighbor-adsorbed oxygen molecules around one edge-state spin and exchange interaction parameter, respectively. Based on the detailed analysis of the observed magnetoresistance, they estimated $\langle z_{\pi\text{-Ox}}J_{\pi\text{-Ox}}\rangle$ to be in the range of ~-6 to -8 K, where $\langle z_{\pi\text{-Ox}}J_{\pi\text{-Ox}}\rangle$ is the average of the parameter $z_{\pi\text{-Ox}}J_{\pi\text{-Ox}}$ randomly varying in space. The strength of the interaction cannot be explained only in terms of the magnetic dipole-dipole interaction, which is in the strength range of ~0.1 K and plays a major role in ordinary magnetic species physisorbed in magnetic hosts. Therefore, it is important to clarify the microscopic origin of its large interaction.

Due to the absence of electric dipole in an oxygen molecule, the electric dipole-dipole interaction cannot be a candidate of the interaction. Therefore, we first focused on the interaction between the electric quadrupole moment Q of an oxygen molecule and electric dipole moment μ of an edge state as a candidate for the interaction (Fig. 2). There should be finite electric dipole moments on the edge sites of the nanographite terminated by functional groups; among these, hydrogen atom is the simplest. The Q-μ interaction is expressed as follows:

$$\hat{H}_{Q-\mu} = \frac{3Q\mu}{2R_{Q-\mu}^4}[\cos\theta_\mu(3\cos^2\theta_Q - 1) - 2\cos\theta_Q\sin\theta_Q\sin\theta_\mu\cos\varphi], \qquad (1)$$

where $R_{Q\text{-}\mu}$, θ_Q, θ_μ, and φ are the absolute value of the distance vector $\boldsymbol{R}_{Q\text{-}\mu}$ between the electric dipole μ and electric quadrupole Q, angle formed by the intersection of the

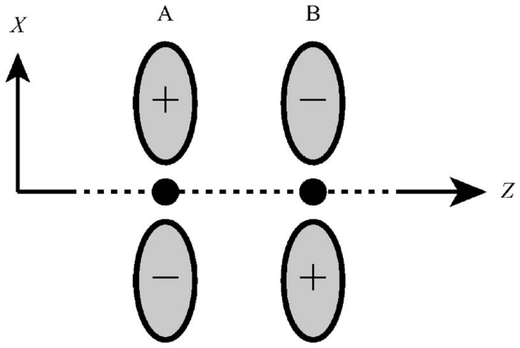

FIG. 3. Antibonding orbital of an oxygen molecule consisting of oxygen atoms A and B. The molecular axis is along the z axis.

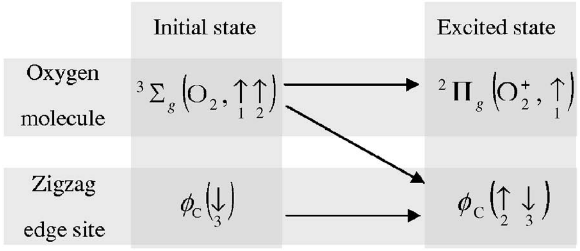

FIG. 4. Second-order perturbation process induced by Hamiltonian $\hat{H}_{Q\text{-}\mu}$ between an oxygen molecule and zigzag edge-state. The three small arrows (up/down) labeled 1, 2, and 3 denote the electron spins.

molecular axis of oxygen with vector $\boldsymbol{R}_{Q\text{-}\mu}$, angle formed by μ with vector $\boldsymbol{R}_{Q\text{-}\mu}$, and difference between the azimuth angles ($\varphi=\varphi_\mu-\varphi_Q$), respectively. Hereafter, we neglect φ by averaging it. Then, Eq. (1) is expressed as follows:

$$\hat{H}_{Q-\mu}=\frac{3Q\mu}{2R_{Q-\mu}^4}\cos\theta_\mu(3\cos^2\theta_Q-1). \tag{2}$$

The electric quadrupole moment is defined as

$$Q=\frac{1}{2}\sum_i e(3\cos^2\vartheta_i-1)r_i^2, \tag{3}$$

where i, e, and ϑ_i are the index of the electron in the oxygen molecule, charge of the electron, and angle formed by position vector $\boldsymbol{r}_i$ of the ith electron with the molecular axis, respectively. The experimental values of Q obtained by the optical birefringence method[20] and microwave collision[21] are -2.82×10^{-25} and -5.3×10^{-27} esu cm^2, respectively. Using geometrical parameters,[22] the calculated value of Q for the oxygen molecule in the ground state ${}^3\Sigma_g$ is estimated to be -2.90×10^{-25} esu cm^2,

$$\left\langle\sum_i y_i^2\right\rangle=\left\langle\sum_i z_i^2\right\rangle=1.68\ \text{Å}^2,\quad \left\langle\sum_i x_i^2\right\rangle=7.71\ \text{Å}^2, \tag{4}$$

this value is in good quantitative agreement with that estimated by the birefringence method. In fact, the observed value derived from the microwave collision is not sufficiently convincing due to the difficulty involved in the experimental technique of the line width measurement in microwave spectrum and subsequent analysis of the measurement. Therefore, for the calculation in this study, we consider the value obtained from the birefringence method.

In the electronic structure of the oxygen molecule expressed as O_2: $[KK(z\sigma)^2(y\sigma)^2(x\sigma)^2(w\pi)^4(v\pi)^2]$, the outermost orbital is an antibonding orbital $(v\pi)^2$ with triplet state ($S=1$) of π_x^*2p,π_y^*2p, where the molecular axis is the z axis shown as Fig. 3. The wave function of the antibonding π_x^*2p is expressed as follows:[23]

$$\psi_g=\phi(A,2p_x)-\phi(B,2p_x), \tag{5}$$

where A and B represent the oxygen atoms constituting an oxygen molecule, as shown in Fig. 3. The wave function of the antibonding π_y^*2p is also expressed in a manner similar to Eq. (5).

The wave function of the edge state localized at the zigzag edge of the nanographene ribbon propagates as $\exp(i\boldsymbol{k}\cdot\boldsymbol{r})u_k(\boldsymbol{r})$ along the direction parallel to the edge. The dispersionless edge-state at the Fermi energy has a δ-function-type density-of-states peak in the region of the wave number $2\pi/3\le|k|\le\pi$, while it extends internally from the zigzag edge as $|k|$ approaches $2\pi/3$. Although we need to discuss the edge state based on such a band model, we consider it to be the local state in order to avoid complexity. In addition, the zigzag edge in actual nanographite domains in ACFs does not have any regular structure, as opposed to that discussed in theory. To simplify the subsequent calculation procedure, a localized wave function $\phi_C\propto\exp(-r/a_C)$ is employed instead of the Wannier function; in this function, a_C is the decay length.

The exchange interaction parameter J is estimated in the second-order perturbation with a perturbed Hamiltonian $\hat{H}_{Q\text{-}\mu}$ of the electric dipole-quadrupole interaction. In this calculation, we consider π electrons localized at the zigzag edge of a nanographite; this edge also functions as an adsorption site for oxygen molecules. Based on the Franck-Condon principle, it is considered that θ_Q, θ_μ, and $\boldsymbol{R}_{Q\text{-}\mu}$ are constant during the electron hopping event. The proposed second-order perturbation process is mediated by the adsorbed oxygen molecule, as shown in Fig. 4. In this process, the electron labeled 2 is transferred from the antibonding orbital $(v\pi)^2$ of the triplet state of an oxygen molecule, wherein highest occupied molecular orbital (HOMOs) ${}^3\Sigma_g(O_2,\underset{1}{\uparrow}\underset{2}{\uparrow})$ are occupied by electrons labeled 1 and 2, to the empty edge state of the zigzag edge. Next, the system returns to the initial state via the inverse process. Based on the doubly degenerate ionized oxygen molecule state ${}^2\Pi_g(O_2^+,\underset{1}{\uparrow})$, Coulomb interaction between a positively ionized oxygen molecule O_2^+ and negatively charged nanographite domain $-e^2/R_{Q\text{-}\mu}$, and energy change in the nanographite domain during the electron hopping event under the assumption that the screening effect is absent, the second-order perturbation energy ΔE_2 is expressed as follows:

$$\Delta E_2 = \frac{2|\langle {}^3\Sigma_g(\mathrm{O}_2, \underset{1\,2}{\uparrow\uparrow}), \phi_C(\underset{3}{\downarrow})|\hat{H}'_{Q-\mu}|{}^2\Pi_g(\mathrm{O}_2^+, \underset{1}{\uparrow}), \phi_C(\underset{2\,3}{\uparrow\downarrow})\rangle|^2}{\{E({}^3\Sigma_g) + E[\phi_C(\underset{3}{\downarrow})]\} - \left\{E({}^2\Pi_g) + E[\phi_C(\underset{2\,3}{\uparrow\downarrow})] - \dfrac{e^2}{R_{Q-\mu}}\right\}}, \qquad (6)$$

where ϕ_C is the wave function localized at the edge site in the nanographite and $E({}^3\Sigma_g)$, $E({}^2\Pi_g)$, $E[\phi_C(\underset{3}{\downarrow})]$, and $E(\phi_C(\underset{2\,3}{\uparrow\downarrow}))$ are the energies of the oxygen molecule in the triplet state ${}^3\Sigma_g$, ionized oxygen molecule (O_2^+) in the doublet state ${}^2\Pi_g$, nanographite before the electron hopping, and nanographite after the electron hopping, respectively. Thus, $\phi_C(\underset{3}{\downarrow})$ and $\phi_C(\underset{2\,3}{\uparrow\downarrow})$ express the doublet state whose HOMO is occupied by the electron labeled 3 and singlet state occupied by electrons labeled 2 and 3, respectively. The denominator of Eq. (6) can be described using the ionization energy $E_{I,O}$ of the oxygen molecule and electron affinity $E_{A,C}$ of the nanographite, these are given by the following relationships:

$$E_{I,O} = E({}^2\Pi_g) - E({}^3\Sigma_g) \quad \text{and } E_{A,C} = E[\phi_C(\underset{3}{\downarrow})] - E[\phi_C(\underset{2\,3}{\uparrow\downarrow})]. \qquad (7)$$

The factor "2" of $|\langle|\hat{H}|\rangle|$ in Eq. (6) is required for the doubly degenerate $(\nu\pi)^2$ of the oxygen molecule. This process is effective only if the distance between the oxygen molecule and zigzag edge is small; this is because an electron belonging to an oxygen molecule in the initial state is transferred to the zigzag site by perturbation $\hat{H}_{Q\text{-}\mu}$, as shown in Eq. (6). In this case, factor $\exp(-2R_{Q\text{-}\mu}/a)$ is required as the overlap of the wave functions between the edge state and oxygen molecule, where $R_{Q\text{-}\mu}$ and a are the distance between the edge state and oxygen molecule and decay length of the wave-function overlap between the zigzag edge and oxygen molecule, respectively, and $R_{Q\text{-}\mu} > a$. If there are $z_{\pi\text{-Ox}}$ number of adsorbed oxygen molecules around the edge state and all the oxygen molecules are assumed to have the sample strength of the interaction, then ΔE_2 is expressed as follows:

$$\Delta E_2 = \frac{2z_{\pi-\mathrm{Ox}} \exp\left(\dfrac{-2R_{Q-\mu}}{a}\right)\left[\dfrac{3Q\mu}{2R_{Q-\mu}^4}\cos\theta_\mu(3\cos^2\theta_Q - 1)\right]^2}{-E_{I,O} + E_{A,C} + \dfrac{e^2}{R_{Q-\mu}}}. \qquad (8)$$

To evaluate the above equation, following parameters are adopted:

$$z_{\pi-\mathrm{Ox}} \sim 4 \quad (\text{Ref. } 24), \quad Q = -2.82 \times 10^{-25}\ \text{esu cm}^2 \quad (\text{Ref. } 20),$$

$$a = 0.2\ \text{nm}, \quad \mu = (1-2) \times 10^{-18}\ \text{esu cm},$$

$$[\cos\theta_\mu(3\cos^2\theta_Q - 1)]^2 \equiv f(\theta_Q, \theta_\mu) = 2,$$

$$E_{I,O} = 12.07\ \text{eV} \quad (\text{Ref. } 25), \quad E_{A,C} = 4.6\ \text{eV}\ (\text{Ref. } 26). \qquad (9)$$

Here, the number of adsorbed oxygen molecules around the edge state ($z_{\pi\text{-Ox}} \sim 4$) is based on the mean of the number of coordinating oxygen molecules to an oxygen molecule adsorbed in ACFs.[24] It is reduced from 6, which is the number of the nearest-neighbor oxygen molecules around an oxygen molecule adsorbed on the graphite plane with a hexagonal regular lattice.[27] The employed decay length—$a \sim 0.2$ nm—is estimated from the sizes of the wave functions of graphitic π-orbital ($a_C \sim 0.17$ nm, obtained from Ref. 28) and oxygen molecules (~ 0.18 nm, obtained from Ref. 22). The estimated value of $[\cos\theta_\mu(3\cos^2\theta_Q - 1)]^2$ is considered to be the intermediate value as it varies between 0 and 4. The electron affinity $E_{A,C}$ of nanographites is assumed to be the same as that of bulk-sized graphite (4.6 eV).[26] The dipole moment at the nanographite edge depends on the type of functional groups bonded to the edge carbon atoms. The plausible functional groups are considered to consist of oxygen, hydrogen, and carbon atoms, in which a phenol group (-OH)[29] with a dipole moment of 1.224×10^{-18} esu cm (Ref. 30) is among the most typical ones, while the dipole moment of C–H and C–O bonds are 0.4 and 0.74×10^{-18} esu cm, respectively. Therefore, we employ $\mu = (1-2) \times 10^{-18}$ esu cm in the calculation in this study.

In this section, we discuss the interaction between the oxygen molecule spin and edge-state spin on the basis of the exchange interaction strength experimentally observed because we do not have any convincing value of the distance between the adsorbed oxygen molecules and carbon atom at the edge-state. Based on the observed strength of $\langle z_{\pi\text{-Ox}} J_{\pi\text{-Ox}} \rangle$ ranging from −6 K to −8 K (Ref. 12), $R_{Q\text{-}\mu}$ is estimated to be 0.45–0.46 and 0.41–0.42 nm for $\mu = 2 \times 10^{-18}$ esu cm and $\mu = 1 \times 10^{-18}$ esu cm, respectively. The DFT calculation of the oxygen molecule adsorbed on the surface of the infinite graphene sheet suggests that the value of $R_{Q\text{-}\mu}$ is in the range of 0.3–0.36 nm (Refs. 31–33), which is smaller than the estimated value of $R_{Q\text{-}\mu}$ by 10%–40%. In the case of the oxygen molecule adsorbed around the edge of the nanographene, wherein the edge-state spins are localized, bulky functional groups bonded to the edge carbon atoms prevent the adsorbed oxygen molecule from approaching the carbon atom. Therefore, the estimated range of values of $R_{Q\text{-}\mu}$ ($\sim$0.41–0.46 nm) is considered to be reasonable for the interaction.

From the above calculation, we can successfully explain the mechanism of the microscopic origin of the antiferromagnetic exchange interaction between the edge-state spin and adsorbed oxygen molecule spin. Eventually, the primary reason for the large $z_{\pi\text{-Ox}} J_{\pi\text{-Ox}}$ is the large electric quadrupole moment Q of the oxygen molecule. At this point, it should be noted that the conventional superexchange interaction, which is operative in most of the existing molecular magnetic systems, cannot contribute to the interaction in this case. This is because the distance $R_{Q\text{-}\mu}$ is too large for the superexchange interaction to operate.

III. HOPPING PROCESS BETWEEN ADJACENT NANOGRAPHITE DOMAINS

In this section, we discuss the electron hopping process between nanographite domains based on the discussion in Sec. II. In particular, we focus on the effect of oxygen adsorption on magnetoresistance. The important conclusion obtained in Sec. II is that the oxygen molecule spins create a strong internal field acting on an edge-state spin via the electric dipole-quadrupole interaction between the edge site of the nanographite and adsorbed oxygen molecule.

The effective field $H_{e,\pi}$ acting on the π-electron spins is operative only when the oxygen molecules are near the edge-state; this field can be expressed as follows:

$$H_{e,\pi} = H + H_{\pi\text{-Ox}} = H + \left[\frac{2}{N_{\text{Ox}}(g_{\text{Ox}}\mu_B)^2} \langle z_{\pi\text{-Ox}} J_{\pi\text{-Ox}} \rangle \right] M_{\text{Ox}}, \tag{10}$$

where H, $H_{\pi\text{-Ox}}$, N_{Ox}, g_{Ox}, μ_B, and M_{Ox} are the applied field, internal field of the oxygen molecules acting on the edge-state spin, number of adsorbed oxygen molecule spins, g value of the oxygen molecule, Bohr magneton, and magnetization of the adsorbed oxygen molecule spins, respectively. The internal field $H_{\pi\text{-Ox}}$ operates antiparallel to the applied field H, as shown in Fig. 5. In a high magnetic field ($\sim$5–10 T), wherein a large magnetoresistance is observed, the Zeeman splitting shown in Fig. 5 satisfies the conditions $\exp(\Delta / k_B T) \gg 1$ and $\exp(\Delta' / k_B T) \gg 1$ for the cases without and with the adsorbed oxygen molecules, respectively. In the above-mentioned conditions, the Zeeman splittings Δ and Δ' for the edge-state spin $s_z = 1/2$ are described in terms of the applied field H and effective field $H_{e,\pi}$ as follows: $\Delta = g_\pi \mu_B H$ and $\Delta' = g_\pi \mu_B H_{e,\pi}$. This is because H and $H_{e,\pi}$ are in the range of $\sim$5–15 T for the corresponding temperatures (2–4 K) considered in this investigation. Under these conditions, the calculated magnetoresistance $\Delta R / R(0)$ is expected to exhibit a strong magnetic-field dependence, as is clarified in the subsequent discussion. At this point, we should take into account the remarks provided by Fujita *et al.*:[1] In a nanographene ribbon, the magnetic moment at each zigzag-edge site (edge-state spin) $m = \langle n_\uparrow \rangle - \langle n_\downarrow \rangle$ is considerably smaller than 1. In the above-mentioned equation, $n_\uparrow$ and $n_\downarrow$ are the occupation probabilities of spin 1/2 and spin −1/2, respectively, on the site. With a decrease in the on-site Coulomb repulsion U, m approaches zero. According to Ref. 1, $m = 0.19\mu_B$ when $U/t = 0.1$ is considered to be the realistic value for nanographene; here, t denotes the transfer integral between the nearest-neighbor carbon atoms. Therefore, we define the effective Bohr magneton $\bar{\mu}_B$ taking into account the factor m($\sim$0.19) as $\bar{\mu}_B = m\mu_B$, and Δ and Δ' are changed to $\Delta = g\bar{\mu}_B H$ and $\Delta' = g\bar{\mu}_B H_{e,\pi}$, respectively.

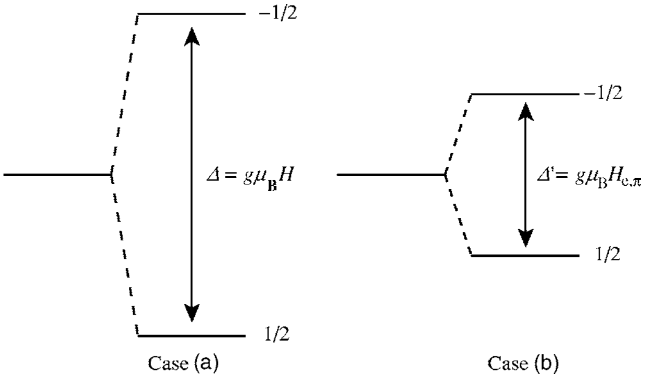

FIG. 5. Zeeman energies of the edge-state spin (a) without and (b) with the adsorbed oxygen molecules. The effective field acting on the edge-state spin is expressed as $H_{e,\pi} = H + H_{\pi\text{-Ox}}$, where $H_{\pi\text{-Ox}}$ is positive when H is negative and vice versa.

Next, we consider the hopping process between two neighboring nanographite domains C and C' wherein the electron i in domain C is transferred to C' for the following cases: (a) without and (b) with the adsorbed oxygen molecules.

Case (a). In this case, the edge-state spin is subjected to only the applied field H because no adsorbed magnetic oxygen molecules exist in the system. In the case of doped semiconductors such as germanium, silicon, and materials derived from them, the Bohr radius is more than 10 nm (Ref. 34). Thus, the overlap of the wave functions governs the electron transport. However, in ACF nanographite networks, the decay length of the wave function of the nonbonding π-electron at the edge-site is in the range of $\sim$0.2 nm, as discussed in Sec. II. Therefore, a long-ranged electric dipole-dipole interaction is required for the electron hopping between nanographite domains. The dipole-dipole interaction is expressed as follows:

$$\hat{H}_{\mu\text{-}\mu} = -\frac{\mu^2}{R^3_{\mu-\mu}}[2\cos\theta_C\cos\theta_{C'} - \sin\theta_C\sin\theta_{C'}\cos(\varphi_C-\varphi_{C'})], \tag{11}$$

where $R_{\mu\text{-}\mu}$, $\theta_{C/C'}$ and $\varphi_{C/C'}$ are the distance between the electric dipoles μ, angle formed by the vector $\boldsymbol{R}_{\mu\text{-}\mu}$ and μ in the nanographite domains C or C', and azimuth angle of μ in the nanographite domains C or C', respectively. The matrix element of $\hat{H}_{\mu\text{-}\mu}$ is obtained as follows:

$$\langle C(\underset{i}{\downarrow})C'(\underset{j}{\uparrow})|\hat{H}_{\mu\text{-}\mu}|C'(\underset{i}{\downarrow}\underset{j}{\uparrow})\rangle = \langle\Phi_{\text{ini}}|\hat{H}_{\mu\text{-}\mu}|\Phi_{\text{fin}}\rangle, \tag{12}$$

where $\underset{i}{\downarrow}$ and $\underset{j}{\uparrow}$ are electrons i and j with down and up spins, respectively. Thus, the probability of hopping W_a is expressed as follows:

$$W_a = \frac{2\pi}{\hbar}|\langle\Phi_{\text{ini}}|\hat{H}_{\mu\text{-}\mu}|\Phi_{\text{fin}}\rangle|^2 n_a(C;\underset{i}{\downarrow})n_a(C';\underset{j}{\uparrow}) \times\frac{1}{\pi}\,\text{Im}\left(E_{\text{ini}}-E_{\text{fin}}-\frac{i\hbar}{2\tau}\right)^{-1}, \tag{13}$$

where E_{ini}, E_{fin}, and τ are the energy of the initial state, energy of the final state, and lifetime of the initial state ($\hbar/2\tau$ refers to the uncertainty energy derived from τ), respectively. If both the nanographite domains C and C' have a zigzag edge, in which a dispersionless edge state exists around the Fermi energy, the electron migration in domain C' occurs smoothly after the electron hopping from C to C'. Therefore, the interdomain hopping process is considered to be the bottle neck in the electron transport. On the other hand, if the nanographite domains have only armchair edges, in which no edge states exist around the Fermi energy, the intradomain electron migration occurs scarcely. Therefore, we consider the zigzag-edge-type nanographite domain.

The occupation probabilities $n_a(C;\underset{i}{\downarrow})$ and $n_a(C';\underset{j}{\uparrow})$ in Eq. (13) are given as follows:

$$n_a(C;\underset{i}{\downarrow}) = \frac{e^{-x}}{e^x+e^{-x}}, \quad n_a(C';\underset{j}{\uparrow}) = \frac{e^{x}}{e^x+e^{-x}}, \tag{14}$$

where

$$x = \frac{1}{2}\frac{g\bar{\mu}_B H}{k_B T}. \tag{15}$$

Further, their product is obtained as follows:

$$n_a(C;\underset{i}{\downarrow})n_a(C';\underset{j}{\uparrow}) = (e^x+e^{-x})^{-2} = (2\cosh x)^{-2}. \tag{16}$$

From Eqs. (11), (13), and (16), the probability of hopping W_a is obtained as follows:

$$W_a = \frac{\pi}{2\hbar}\left[\frac{\mu^2}{R^3_{\mu-\mu}}\exp\left(-\frac{R_{\mu-\mu}}{a_C}\right)\right]^2 G(\theta_C,\theta_{C'},\varphi_C,\varphi_{C'}) \times(\cosh x)^{-2}\frac{1}{\pi}\,\text{Im}\left(E_{\text{ini}}-E_{\text{fin}}-\frac{i\hbar}{2\tau}\right)^{-1},$$

$$G(\theta_C,\theta_{C'},\varphi_C,\varphi_{C'}) \equiv [2\cos\theta_C\cos\theta_{C'} - \sin\theta_C\sin\theta_{C'}\cos(\varphi_C-\varphi_{C'})]^2. \tag{17}$$

The factor $\exp(-2R_{\mu\text{-}\mu}/a_C)$ in Eq. (17) is similar to that appearing in Eq. (8) by taking into account the decay in the overlap of the wave functions.

Next, we estimate the strength $|\langle\Phi_{\text{ini}}|\hat{H}_{\mu\text{-}\mu}|\Phi_{\text{fin}}\rangle|^2$, which is the remaining contribution in W_a after $\pi/2\hbar(\cosh x)^{-2}(1/\pi)\text{Im}[E_{\text{ini}}-E_{\text{fin}}-(i\hbar/2\tau)]^{-1}$ is eliminated from Eq. (17). To evaluate $|\langle\Phi_{\text{ini}}|\hat{H}_{\mu\text{-}\mu}|\Phi_{\text{fin}}\rangle|$, the intermediate value $G(\theta_C,\theta_{C'},\varphi_C,\varphi_{C'})=2$ is employed for $G(\theta_C,\theta_{C'},\varphi_C,\varphi_{C'})$ as it varies between 0 and 4. $R_{\mu\text{-}\mu}$ corresponds to the inter-edge-state distance between adjacent nanographite domains. By taking into account that the nanopore size is estimated to be ~1 nm (Ref. 35) and sizes of the functional groups at the edge-site are deduced to be ~0.2–0.3 nm (note that the C–O–H bond length for phenol is ~0.23 nm), we estimate that $R_{\mu\text{-}\mu}$=0.75 nm. Subsequently,

$$|\langle\Phi_{\text{ini}}|\hat{H}_{\mu-\mu}|\Phi_{\text{fin}}\rangle| = 2.3\text{ K}. \tag{18}$$

Case (b). The calculation in this case is performed in a manner similar to that of case (a). For simplification, we postulate that both the edge-state spins on the different nanographite domains C and C', between which the interdomain hopping occurs, are affected by the oxygen molecule under the same condition and subjected to the same effective field $H_{e,\pi}$. From a practical viewpoint, it is reasonable to consider that the effective fields acting on the edge-state spins of different nanographite domains are not the same. Owing to the above postulation, we derive a formula facilitating the comparison between the calculated and experimental values. Furthermore, in case (b), it is hypothesized that there exist a few hopping processes that are not subjected to the effect of the oxygen molecule spin, similar to case (a), but the number of such processes might be negligibly small. Based on this simplification, W_b is obtained as follows:

$$W_b = \frac{\pi}{2\hbar}\left[\frac{\mu^2}{R^3_{\mu-\mu}}\exp\left(-\frac{R_{\mu-\mu}}{a_C}\right)\right]^2 G(\theta_C,\theta_{C'},\varphi_C,\varphi_{C'}) \times(\cosh x')^{-2}\frac{1}{\pi}\,\text{Im}\left(E_{\text{ini}}-E_{\text{fin}}-\frac{i\hbar}{2\tau}\right)^{-1}. \tag{19}$$

By substituting n_b for n_a in Eq. (17), we get $n_b(C;\underset{i}{\downarrow})=e^{-x'}/(e^{x'}+e^{-x'})$ and $n_b(C';\underset{j}{\uparrow})=e^{x'}/(e^{x'}+e^{-x'})$, where x' is expressed as follows:

$$x' = \frac{1}{2}\frac{g\bar{\mu}_B H_{e,\pi}}{k_B T}. \tag{20}$$

$|\langle\Phi_{\text{ini}}|\hat{H}_{\mu\text{-}\mu}|\Phi_{\text{fin}}\rangle|^2 G(\phi_c,\phi_c,\varphi_c,\varphi_{c'})(1/\pi)\text{Im}[E_{\text{ini}}-E_{\text{fin}}-(i\hbar/2\tau)]^{-1}$ is common to both W_a and W_b. Electrical resistance R is proportional to the inverse of the probability of hopping W_a and W_b. Therefore, the ratio of $R(H)/R(0)$ be-

TABLE I. Comparison of the calculated and experimental values at 2.19 K. The experimental values are obtained from Ref. 12.

(a)	Theory (m=0.19)			Theory (m=0.3)		
H (T)	$\cosh^2 x$	$\cosh^2 x'$	$(\cosh x/\cosh x')^2$	$\cosh^2 x$	$\cosh^2 x'$	$(\cosh x/\cosh x')^2$
15.0	1.98	1.44	1.38	4.46	2.30	1.94
12.4	1.62	1.29	1.26	2.97	1.81	1.65
10	1.38	1.18	1.18	2.13	1.48	1.44
7.5	1.20	1.09	1.10	1.55	1.23	1.26
5.0	1.09	1.04	1.05	1.23	1.09	1.13

(b)	Experiment		
H (T)	$[R(H)/R(0)]_a$	$[R(H)/R(0)]_b$	$r_{a/b}$
15.0	7.57	3.86	1.96
12.4	5.17	2.83	1.83
10	3.51	2.11	1.67
7.5	2.27	1.57	1.45
5.0	1.56	1.24	1.26

tween cases (a) and (b), referred to as $r_{a/b}$, is expressed as follows:

$$r_{a/b} \equiv \frac{[R(H)/R(0)]_a}{[R(H)/R(0)]_b} \cong \left(\frac{W_a}{W_b}\right)^{-1} = \left[\frac{\cosh x}{\cosh x'}\right]^2. \qquad (21)$$

Using Eq. (21), the calculated values of $[\cosh x/\cosh x']^2$ and their magnetic-field dependence can be compared with the experimental values. These results are summarized in Table I. It should be noted that in Eq. (21), x contains m and x' contains m and $H_{\pi\text{-Ox}}$ as parameters. We adopt the experimentally obtained value of $H_{\pi\text{-Ox}}$ (Ref. 12) and m=0.19 (Ref. 1). Due to the relatively poor approximation under the weak magnetic field considered in our theory, it would be reasonable to compare the calculated and experimental values in the $H > 5$ T region. In Table I, the calculated value of $(W_a/W_b)^{-2}$ is in qualitative agreement with the experimental value of $r_{a/b}$, and $[R(H)/R(0)]_a$ and $[R(H)/R(0)]_b$ are almost proportional to $\cosh^2 x$ and $\cosh^2 x'$, respectively. Further, the employment of m=0.30 instead of 0.19 can provide better fitting to the experimental values. These results endorse the validity of our calculation model.

IV. SUMMARY

The objective of this study is to present a theoretical clarification for the microscopic mechanism of the interaction between the adsorbed oxygen molecule spin and edge-state spin of nanographites and electron hopping in nanographite networks. Using the proposed theory, the magnetoresistance behavior can be well explained in relation to the physisorption of guest molecules, especially for adsorbed magnetic oxygen molecules. The obtained results are summarized as follows:

It is proved that the electric dipole-quadrupole interaction between the edge-site of the nanographite and adsorbed oxygen molecule is the origin of the large exchange interaction between them. This implies that the spin of the adsorbed oxygen molecule works to reduce the effective field acting on the edge-state spin via antiferromagnetic coupling. As a result, in spin-polarization-dependent hopping processes, the magnetoresistance in the oxygen-adsorbed state is lesser than that in the non-adsorbed or non-magnetic-molecule-adsorbed state (argon, nitrogen, or helium).

The hopping process between adjacent nanographite domains is governed by electric dipole-dipole interaction. The result that the amplitude of the edge-state spin is smaller than μ_B, suggested by M. Fujita *et al.*,[1] plays an important role in explaining the amplitude and magnetic-field dependence of the observed magnetoresistance.

ACKNOWLEDGMENTS

One of the authors (K.S.) would like to express his sincere thanks to Miho Sugihara for her valuable discussion. This work was supported by a Grant-in-Aid for Scientific Research No. 15105005 from the Japan Society for the Promotion of Science (JSPS).

---

[1] M. Fujita, K. Wakabayashi, K. Nakata, and K. Kusakabe, J. Phys. Soc. Jpn. **65**, 1920 (1996).

[2] K. Wakabayashi, M. Fujita, H. Ajiki, and M. Sigrist, Phys. Rev. B **59**, 8271 (1999).

[3] Y. Kobayashi, K. Fukui, T. Enoki, K. Kusakabe, and Y. Kaburagi, Phys. Rev. B **71**, 193406 (2005).

[4] Y. Kobayashi, K. Fukui, T. Enoki, and K. Kusakabe, Phys. Rev. B **73**, 125415 (2006).

[5] T. Enoki and Y. Kobayashi, J. Mater. Chem. **15**, 3999 (2005).

[6] K. Kusakabe and M. Maruyama, Phys. Rev. B **67**, 092406 (2003).

[7] J. Kondo, *Solid State Physics* (Academic, New York, 1969), Vol. 23.

[8] M. N. Baibich, J. M. Broto, A. Fert, F. Nguyen Van Dau, F. Petroff, P. Etienne, G. Creuzet, A. Friederich, and J. Chazelas, Phys. Rev. Lett. **61**, 2472 (1988).

[9] Y. Shibayama, H. Sato, T. Enoki, X. Bi, M. S. Dresselhaus, and M. Endo, J. Phys. Soc. Jpn. **69**, 754 (2000).

[10] Y. Shibayama, H. Sato, T. Enoki, and M. Endo, Phys. Rev. Lett. **84**, 1744 (2000).

[11] A. W. P. Fung, M. S. Dresselhaus, and M. Endo, Phys. Rev. B **48**, 14953 (1993).

[12] K. Takahara, K. Takai, T. Enoki, and K. Sugihara, Phys. Rev. B (to be published).

[13] A. Nakayama, K. Suzuki, T. Enoki, C. Ishii, K. Kaneko, M. Endo, and N. Shindo, Solid State Commun. **93**, 323 (1995).

[14] N. Kobayashi, T. Enoki, C. Ishii, K. Kaneko, and M. Endo, J. Chem. Phys. **109**, 1983 (1998).

[15] H. Sato, N. Kawatsu, T. Enoki, M. Endo, R. Kobori, S. Maruyama, and K. Kaneko, Solid State Commun. **125**, 641 (2003).

[16] K. Takai, H. Kumagai, H. Sato, and T. Enoki, Phys. Rev. B **73**, 35435 (2006).

[17] K. Sugihara, A. Nakayama, and T. Enoki, J. Phys. Soc. Jpn. **64**, 2614 (1995).

[18] A. Kurobe and H. Kamimura, J. Phys. Soc. Jpn. **51**, 1904 (1982).

[19] M. Pollak and B. I. Shklovskii, *Hopping Transport in Solids-Modern Problems in Condensed Matter Sciences* (North-Holland, New York, 1991).

[20] A. D. Buckingham, Chem. Br. **1**, 54 (1965); T. A. Miller, J. Chem. Phys. **54**, 330 (1971).

[21] J. O. Hirschfelder, C. F. Curtiss, and R. B. Bird, *Molecular Theory of Gases and Liquids* (Wiley, New York, 1964).

[22] M. Kotani, Y. Mizuno, K. Kayama, and E. Ishiguro, J. Phys. Soc. Jpn. **12**, 707 (1957).

[23] C. A. Coulson, *Valence* (Oxford University Press, London, 1963).

[24] T. Enoki, *Hyoumen* **34**, 311 (1996).

[25] S. G. Lias, J. E. Bartmess, J. F. Liebman, J. L. Holmes, R. D. Levin, and W. G. Mallard, J. Phys. Chem. Ref. Data **17**, suppl.1 (1988).

[26] B. T. Kelly, *Physics of Graphite* (Applied Science, London, 1981).

[27] H. Suematsu and Y. Murakami, J. Magn. Magn. Mater. **90-91**, 749 (1990).

[28] F. A. Cotton, G. Wilinson, and P. L. Gaus, *Basic Inorganic Chemistry*, 3rd ed. (Wiley, New York, 1999).

[29] Z. R. Yue, W. Jiang, L. Wang, S. D. Gardner, and C. U. Pittman, Jr., Carbon **37**, 1785 (1999).

[30] D. R. Lide, *CRC Handbook of Chemistry and Physics*, 81st ed. (CRC, Boca Raton, 2000).

[31] D. C. Sorescu, K. D. Jordan, and P. Avouris, J. Phys. Chem. B **105**, 11227 (2001).

[32] P. Giannozzi, R. Car, and G. Scoles, J. Chem. Phys. **118**, 1003 (2003).

[33] Y. J. Xu and J. Q. Li, Chem. Phys. Lett. **400**, 406 (2004).

[34] B. I. Shklovskii and A. L. Efros, *Electronic Properties of Doped Semiconductors*, Springer Series in Solid-State Sciences Vol. 45 (Springer, Berlin, 1984).

[35] H. Kanoh, A. Zamma, N. Setoyama, Y. Hanzawa, and K. Kaneko, Langmuir **13**, 1047 (1997).